Can we design transcranial acoustic holograms without ionizing radiation?

Alba Eroles-Simó*,Víctor Vegas-Luque*, Alicia Carrión*, José A. Pineda-Pardo†, Francisco Camarena*, Noé Jiménez*

*Instituto de Instrumentación para Imagen Molecular, Universitat Politècnica de València / CSIC, Valencia, Spain

†HM CINAC (Centro Integral de Neurociencias Abarca Campal), Hospital Universitario HM Puerta del Sur, HM Hospitales, Madrid, Spain

2025 IEEE International Ultrasonics Symposium (IUS) | 979-8-3315-2332-9/25/$31.00 ©2025 IEEE | DOI: 10.1109/IUS62464.2025.11201759

***Abstract*—Acoustic holography is a promising technique in transcranial therapeutic ultrasound, enabling precise wavefront shaping to compensate skull-induced aberrations using single-element transducers. Traditionally, the design of these holograms has relied on full-wave simulations based on acoustic properties extracted from computed tomography (CT), exposing the patient to ionizing radiation. In this study, we present a radiation-free alternative by employing Zero Echo Time (ZTE) magnetic resonance imaging (MRI), capable of capturing signal from bone tissue. By establishing a linear correlation between ZTE intensity values and CT Hounsfield units, we generate pseudo-CT images suitable for acoustic simulation. Simulated results on 5 patients demonstrate that holograms based on pseudo-CT data achieve a peak pressure at focus with mean reduction of 5.38% and about 1 mm spatial deviation respect to those obtained using CT data. This approach provides a viable pathway for implementing safe, patient-specific, wearable holographic systems for transcranial ultrasound therapy without the need of ionizing radiation.**

***Index Terms*—Transcranial Therapeutic Ultrasound, Acoustic Holography, Zero Echo Time.**

I. Introduction

Therapeutic ultrasound is a minimally invasive technique that enables the precise targeting of brain structures, offering promising applications in the treatment of central nervous system disorders [1]. However, skull induces aberrations, attenuation and beam defocusing due to its high impedance, heterogeneity and complex morphology. To overcome these limitations, acoustic holograms have been proposed. These 3D-printed passive lenses are placed over single element transducers and can encode complex wavefronts to produce arbitrary fields. In addition, acoustic holograms can locally modulate the phase of the ultrasound beam to correct skull-induced aberrations and focus on the desired brain regions [2]. These devices have been proposed for several applications like localized drug delivery [3], local passive cavitation monitoring [4], generating thermal patterns for localized hyperthermia [5], generating complex fields like vortices for particle trapping [6], or to control scattering to improve ultrafast imaging [7].

For transcranial ultrasound, the design of acoustic holograms requires full-wave simulations based on the acoustic properties of the tissues of each patient. The critical magnitudes are the sound speed and density of the human skull bones. Those properties are typically obtained from computed tomography (CT) [8]. However, CT exposes patients to ionizing radiation, which is undesirable. For phased-arrays, pseudo-CT obtained by magnetic resonance imaging (MRI) have been proposed in the past by using T1-weighted MRI [9]. However, in T1-weighted images, signal acquisition begins after a delay (echo time, TE), which causes the rapidly decaying signals from bone to disappear before they can be captured, leading to bone appearing signal void (dark), making it difficult to extract accurate anatomical or density information. On the other hand, Zero Echo Time (ZTE) MRI enables signal acquisition almost immediately after radio-frequency excitation, allowing detection of fast-decaying signal from bone tissues [10]. This results in high-contrast images where bone is clearly visible, enabling the generation of pseudo-CTs that closely match the spatial and density distribution of actual CT scans [11]. In this study, we propose the use of ZTE-MRI as a radiation-free alternative for hologram design.

II. Materials and Methods

A. CT and ZTE images

CT and ZTE images used in this work were obtained and provided by the Centro Integral de Neurociencias A.C. (HM CINAC) in Hospital Universitario HM Puerta del Sur (Madrid, Spain), all patients provided written consent for data collection. The registration of both images is performed using the software 3DSlicer. The gold standard density and sound velocity of hard and soft tissues are obtained from HU intensity values in CT considering X-ray attenuation.

Following the methodology proposed by Miscouridou *et al.* [11], ZTE images are post-processed using a bias-field correction filter to compensate for intensity inhomogeneities. Voxel intensities are normalized relative to the soft tissue peak to ensure consistent scaling across datasets. A threshold is then applied to the normalized ZTE image to generate a binary skull mask, which is refined using morphological operations to fill gaps and ensure mask continuity. This mask is used to identify the voxels for which the linear regression $HU_{CT} = -2085 \cdot ZTE - 2329$ is applied in order to generate

Authorized licensed use limited to: UNIVERSIDAD POLITECNICA DE VALENCIA. Downloaded on October 27,2025 at 10:46:57 UTC from IEEE Xplore. Restrictions apply.

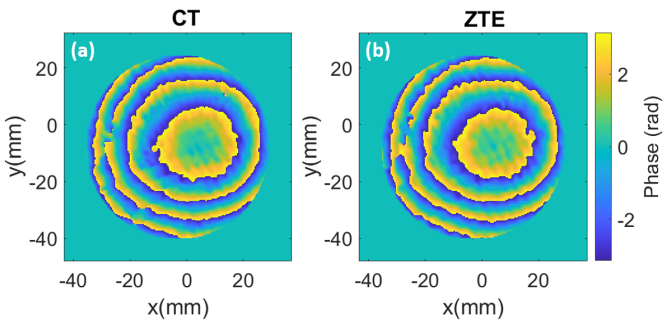


Fig. 1. Phase distribution of the wavefront recorded over the holographic plane coming from the virtual source, taking into account the acoustic properties of (a) the CT image and (b) the pseudo-CT image.

pseudo-CT images, where HU_{CT} are the pseudo-CT values in Hounsfield units and ZTE is the intensity of the processed ZTE data.

B. Acoustic simulations

A flat circular single-element transducer with a diameter of 65 mm and a central frequency of 650 kHz placed over the temporal bone window is used for acoustic simulations. Those are performed in the time domain using Matlab k-Wave toolbox, which employs a pseudo-spectral time-domain simulation method in k-space to model ultrasound propagation in heterogeneous media. To design the hologram, a virtual source is placed at the center of the therapeutic structure, the ventralis intermedius nucleus (VIM), previously segmented and registered for each subject. It emits a 100-cycle sinusoidal pulse at the central frequency of the transducer. As the wave propagates through the skull, it undergoes distortion due to differences in sound speed, density and attenuation, relative to those of soft tissues. The resulting wavefront is captured on the holographic plane; the phase distribution is used to design the geometry of the acoustic lens. Two simulations are performed, one using CT-derived acoustic properties and the other, using pseudo-CT data. This yields two sets of personalized acoustic holograms, as Fig. 1 shows.

A second simulation is performed to evaluate the focusing performance of the designed holographic lenses. The same acoustic wave is now emitted from the transducer, it propagates through the holographic lens, which modulates its phase, and then through the skull, enabling the focalization over the desired structure. The resulting pressure field is recorded for analysis. In the first situation, the lens designed using CT-derived acoustic properties is evaluated under matching conditions (CT-CT). In the second situation, pseudo-CT based lens performance is evaluated under CT acoustic properties in an effort to approximate the most realistic clinical scenario (ZTE-CT).

III. Results

The acoustic fields obtained considering the holographic lens designed using CT and ZTE derived acoustic properties

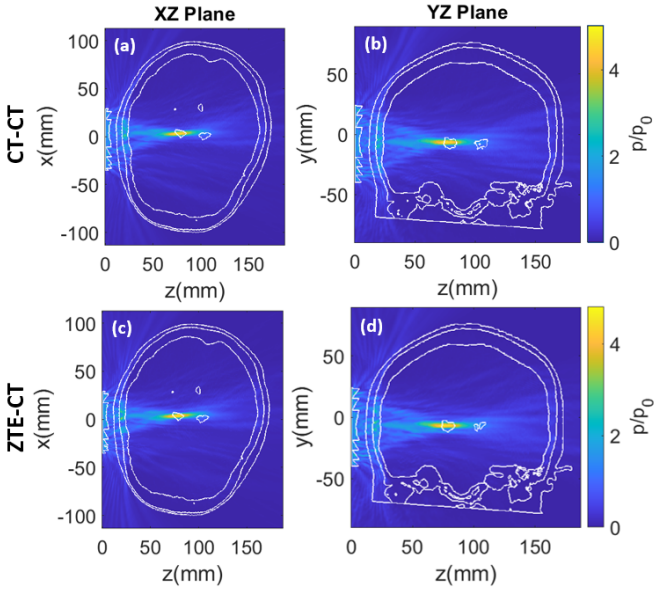


Fig. 2. Simulated field XY and YZ planes amplitude distribution of acoustic field. (a) and (b) for the CT-CT simulation conditions, (c) and (d) for ZTE-CT conditions.

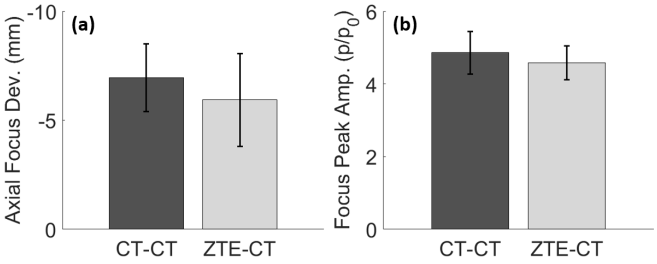


Fig. 3. (a) Mean focus deviation in the beam propagation axis. (b) Mean normalized peak pressure measured at the beam, focus. Kologorov-Smirnov test ($p<0.05$), establishes that there is no significant difference between CT-CT and ZTE-CT.

are evaluated in 5 anonymized patients. In Fig. 2, the resulting acoustic fields obtained in the different considered situations for a particular patient are analyzed, being (a) and (b) XZ and YZ plans for CT-CT, and (c) and (d) for ZTE-CT, respectively. The differences between the resulting acoustic fields are quantified in terms of variations in focal position and peak pressure at the focus. Fig. 3 (a) illustrates the deviation along the axial axis with respect to the coordinates of the virtual source defined for the holographic lens design, establishing that there is no significant difference between simulation conditions. A deviation of 1.02 ± 1.97 mm along the beam propagation axis is observed between CT-CT and ZTE-CT simulations. Regarding pressure values, a decrease of 5.38% in the maximum focal pressure is observed in ZTE-CT field compared to CT-CT field. Fig. 3 (b) presents the mean maximum pressure measured at the focus for the 5 anonymized patients under each simulation condition.

Authorized licensed use limited to: UNIVERSIDAD POLITECNICA DE VALENCIA. Downloaded on October 27,2025 at 10:46:57 UTC from IEEE Xplore. Restrictions apply.

IV. Conclusions

Using ZTE-MRI data, pseudo-CT images are generated to accurately estimate skull acoustic properties, enabling the design of subject-specific holographic lenses. Comparative analyses of the acoustic fields obtained by CT-based and pseudo-CT based lens demonstrate minimal discrepancies in focal location and peak pressure amplitudes. These results validate the feasibility of ZTE-MRI as a non-ionizing alternative to CT for patient specific hologram generation.

V. Acknowledgments

This research has been founded by Generalitat Valenciana through grants INVEST/2023/553, EDGJID/2021/189, INNEST/2022/345 and CIAICO/2023/052. This research has been founded by the Ministerio Español de Ciencia e Innovación y el Ministerio de Universidades with grants PREP2022-000156 by the Agencia Estatal de Investigación, PID2022-142719OB-C21 and CNS2023-145707 founded by MCIN/AEI/10.13039/501100011033 and by the FSE+.

References

[1] K. Lee, T. Y. Park, W. Lee, and H. Kim, "A review of functional neuromodulation in humans using low-intensity transcranial focused ultrasound," *Biomedical engineering letters*, vol. 14, no. 3, pp. 407–438, 2024.

[2] S. Jiménez-Gambín, N. Jiménez, J. M. Benlloch, and F. Camarena, "Holograms to focus arbitrary ultrasonic fields through the skull," *Physical Review Applied*, vol. 12, no. 1, p. 014016, 2019.

[3] S. Jiménez-Gambín, N. Jiménez, A. N. Pouliopoulos, J. M. Benlloch, E. E. Konofagou, and F. Camarena, "Acoustic holograms for bilateral blood-brain barrier opening in a mouse model," *IEEE Transactions on Biomedical Engineering*, vol. 69, no. 4, pp. 1359–1368, 2021.

[4] N. Lamothe, D. Andrés, A. Carrión, F. Camarena, J. A. Pineda-Pardo, and N. Jiménez, "Monitoring holograms for therapeutic ultrasound using passive cavitation beamforming," *Applied Acoustics*, vol. 224, p. 110144, 2024.

[5] D. Andrés, J. Vappou, N. Jiménez, and F. Camarena, "Thermal holographic patterns for ultrasound hyperthermia," *Applied Physics Letters*, vol. 120, no. 8, 2022.

[6] S. Jiménez-Gambín, N. Jiménez, and F. Camarena, "Transcranial focusing of ultrasonic vortices by acoustic holograms," *Physical Review Applied*, vol. 14, no. 5, p. 054070, 2020.

[7] E. Ballestero, J. Rodriguez-Sendra, V. Romero-García, J.-P. Groby, and N. Jiménez, "Bidirectional lambertian scatterers using acoustic holograms for the simultaneous control of reflected and transmitted wavefronts," *Advanced Functional Materials*, p. 2423715, 2025.

[8] J.-F. Aubry, M. Tanter, M. Pernot, J.-L. Thomas, and M. Fink, "Experimental demonstration of noninvasive transskull adaptive focusing based on prior computed tomography scans," *The Journal of the Acoustical Society of America*, vol. 113, no. 1, pp. 84–93, 2003.

[9] M. Wintermark, N. J. Tustison, W. J. Elias, J. T. Patrie, W. Xin, N. Demartini, M. Eames, S. Sumer, B. Lau, A. Cupino, *et al.*, "T1-weighted MRI as a substitute to CT for refocusing planning in MR-guided focused ultrasound," *Physics in Medicine & Biology*, vol. 59, no. 13, p. 3599, 2014.

[10] F. Wiesinger, L. I. Sacolick, A. Menini, S. S. Kaushik, S. Ahn, P. Veit-Haibach, G. Delso, and D. D. Shanbhag, "Zero TE MR bone imaging in the head," *Magnetic resonance in medicine*, vol. 75, no. 1, pp. 107–114, 2016.

[11] M. Miscouridou, J. A. Pineda-Pardo, C. J. Stagg, B. E. Treeby, and A. Stanziola, "Classical and learned MR to pseudo-CT mappings for accurate transcranial ultrasound simulation," *IEEE transactions on ultrasonics, ferroelectrics, and frequency control*, vol. 69, no. 10, pp. 2896–2905, 2022.

Authorized licensed use limited to: UNIVERSIDAD POLITECNICA DE VALENCIA. Downloaded on October 27,2025 at 10:46:57 UTC from IEEE Xplore. Restrictions apply.